28 Apr 1981, 9:00 am - 12:30 pm

Dynamic Behaviour of Sandy Soil and Liquefaction

Tadanobu Sato
Kyoto University, Japan

Toru Shibata
Kyoto University, Japan

Ryoji Ito
Shimizu Kensetsu Co. Ltd., Japan

Proceedings: First International Conference on Recent Advances in Geotechnical Earthquake Engineering and Soil Dynamics, April 26 - May 3, 1981, St. Louis, Missouri

Dynamic Behaviour of Sandy Soil and Liquefaction

Tadanobu Sato, Associate Professor
Toru Shibata, Professor
Disaster Prevention Research Institute, Kyoto University, Uji, Kyoto, Japan

Ryoji Ito, Construction Engineer
Shimizu Kensetsu Co. Ltd., Tokyo, Japan

SYNOPSIS A mathematical model is formulated to present constitutive relation of sandy soil under cyclic loading. The fundamental concepts of kinematic and isotropic work-hardening plasticity theory are utilized here to obtain the relationship between rate of strain and rate of stress, in which the yield function, hardening function and plastic potential are proposed from experimental evidence and theoretical considerations. The predicted inelastic behaviour is compared with available experimental results of conventional cyclic triaxial tests, paticularly of liquefaction phenomena.

INTRODUCTION

The object of this paper is to make clear the stress-strain characteristics of sandy soil under cyclic and transient loading which will permit non-linear analysis while taking account of liquefaction phenomena. The prediction of stress-strain behaviour of soil based on the theory of plasticity has been developed by Roscoe's research group[1] using the concept of associated flow rule, whereas there has been another approach based on the non-associated flow rule. However, it has been difficult to present the deformation characteristics under cyclic loading condition because these theories have treated only the monotonic loading conditon. To remove this difficulty the plasticity theory, considering the kinematic work-hardening concepts, has been applied to the soil behaviour by several authors.[2] In this paper, we propose a more realistic constitutive law based on the experimental results and the kinematic work-hardening plasticity theory.

To verify the theory it is necessary to measure the behaviour of sandy soil under small strain accurately. We put a load cell into the triaxial cell and placed two non-contact deformation sensors at both sides of the piston to measure the strain of order 10^{-5}. The saturated test samples are formed in a cylindrical mold and frozen for ease of setting.

A STRESS-STRAIN RELATIONSHIP

The plastic strain increment is calculated based on the non-associated flow rule proposed by Hill:[3]

$$d\varepsilon^{p}_{ij} = h \frac{\partial g}{\partial \sigma_{ij}} df \qquad (1)$$

where ε^{p}_{ij} and σ_{ij} are plastic strain and stress tensors h is a hardening function, g is a plastic potential and df is the total derivative of the function f which defines the yield locus.

The following explanations provide information for the functions f, g and h.

(1) Yield Function

The yielding behaviour for shear deformation and consolidation can be treated independently, and the functions f^{*}_{s} and f^{*}_{c} specifying a yield locus for shear and consolidation are given as follows:

$$f^{*}_{s} = f_{s} - f_{sy} = 0 \qquad f^{*}_{c} = \sigma'_{m} - \sigma_{my} = 0 \qquad (2)$$

where $f_s = \eta = (\tau_{oct}/\sigma'_m)$, $f_{sy} = \eta^{\pm}_{y} = (\tau_{oct}/\sigma'_m)^{\pm}_{y}$, σ'_m is the effective mean stress, f_{sy} and σ_{my} are hardening parameters for shear and consoildation, respectively.

The octahedral shear stress τ_{oct} and strain γ_{oct} are positive definite variables, therefore, the ratio η is positive for compression and extension. To explain the dilatancy phenomenon of sand for both compression and extension it is necessary to define a negative η. We treat the η-γ_{oct} relation as shown in Fig.1 as having the meaning in the negative η and γ_{oct} domain.

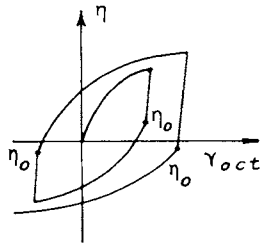

Fig.1 η-γ_{oct} Relation

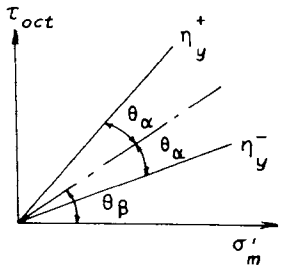

Fig.2 Yield Function

The yield surface for shear being assumed as a circular cone in τ_{oct}-σ'_m space moves in the stress space as expanding. Fig.2 shows the yield surface. Innerpart enclosed by the yield surface η^{+}_{y} and η^{-}_{y} is the elastic region. The kinematic hardening is expressed by the movement of the center axis of the cone and the enlargement of the conic angle is taken as the measure of the isotropic hardening. Using the notations shown in the figure the hardening parameters for shear deformation are given as follows:

$$\eta^{\pm}_{y} = \tan(\theta_{\alpha} \pm \theta_{\beta}) = \frac{\alpha \pm \beta}{1 \mp \alpha\beta} \qquad (3)$$

$$\alpha = \tan\theta_{\alpha} \qquad \beta = \tan\theta_{\beta}$$

where α and β are measures of the isotropic and kinematic hardening, respectively.

(2) Plastic Potential

The plastic potential g_c for consolidation process is given by

$$g_c = \sigma'_m \qquad (4)$$

The potential has meaning only of the condition $f_c - f_{cy} = 0$ and $df_c > 0$ are satisfied.

The plastic potential g_s for shearing process (in which $f_s - f_{sy} = 0$ and $df_s > 0$ are satisfied) and its partial derivative with respect to τ_{oct} and σ'_m are derived from the relationship between the effective stress ratio η and the strain increment ratio $dv^p_d / d\gamma^p_{oct}$ (called the stress-dilatancy relation).

$$\frac{\tau_{oct}}{\sigma'_m} = AM_m - \frac{2}{3}B\frac{dv^p_d}{d\gamma^p_{oct}} \qquad (5)$$

and the assumption of the normality rule

$$\frac{d\tau_{oct}}{d\sigma'_m} = -\frac{2}{3}\frac{dv^p_d}{d\gamma^p_{oct}} \qquad (6)$$

where dv^p_d is the volumetric strain increment due to dilatancy.

Substituting Eq.(5) into Eq.(6), we can get the differential equation of plastic potential as follows:

$$d\tau_{oct} + B(AM_m - \eta)d\sigma'_m = 0 \qquad (7)$$

Comparing this equation with the total derivative of the plastic potential function, the partial derivatives of plastic potential are calculated as follows:

$$\frac{\partial g_s}{\partial \tau_{oct}} = 1 \qquad (8) \qquad \frac{\partial g_s}{\partial \sigma'_m} = B(AM_m - \eta) \qquad (9)$$

$$B = \begin{cases} 1 & |\eta_o| > M_m \text{ or} \\ & |\eta_o| < M_m \text{ and } |\eta| > M_m \\ \left(\dfrac{AM_m}{AM_m - \eta_o}\right)^2 & \text{except above} \\ & \eta,\ \eta_o \text{ domain} \end{cases} \qquad (10)$$

where M_m is the value of τ_{oct}/σ'_m at dv^p_d being equal to zero, A is +1 for loading towards the critical state in compression ($d\eta > 0$) and -1 for extension ($d\eta < 0$), and η_o is the effective stress ratio at which the plastic strain becomes predominant in the cyclic loading condition as shown in Fig.1.

The general view of the stress dilatancy relation given by Eq.(5) and accompanying undrained stress path were given in Ref.(4). A brief explanation, however, is given in Fig.3. If the effective stress ratio is smaller than M_m and its initial value η_o is on the compression side, the stress-dilatancy relation is expressed by the line ① above the dashed line, which expresses the stress dilatancy relation for normally consolidated sand. On the other hand, if the initial value η_o is on the extension side, the stress dilatancy relation is expressed by the line ② below the dashed line. The symbols in the figure show the experimental results. These results are consistent with that the slope of the undrained stress path in the case of ② is steeper than that of a normally consolidated sand, on the contrary, in the case of ① its slope becomes gentle. The parameter B in Eq.(10), therefore, contains the effect of anisotropic consolidation.

(3) The Isotropic Hardening Rule

We assume an exponential function of γ^p_{oct} for the isotropic hardening parameter α. On the drained condition, α increases until the region enclosed by the compression and extension failure line (M_{fcomp} and M_{fext}) becomes a perfectly elastic state. On the undrained condition, assuming the softening behaviour cased by the liquefaction as the decrease of the elastic region, α decreases sharply when the effective stress ratio is beyond the M_m-line. Depending on these assumption, the following functions of α are defined.

I. In the case that the elastic region expands

$$\alpha = \alpha_o + (\alpha_f - \alpha_o)\{1 - \exp(-\frac{\xi_o}{\alpha_f}|\gamma^p_{oct} - \gamma_o|)\}$$

$$\xi = \xi_o \exp(-\frac{\xi_o}{\alpha_f}\gamma_o) \qquad (11)$$

II. In the case that the elastic region shrinks (This has a meaning only for the case of undrained and $|\eta| > M_m$ conditions)

$$\alpha = \alpha_m \exp(-\frac{\xi^*_o}{\alpha_f}|\gamma^p_{oct} - \gamma_m|) \qquad (12)$$

where α_o is the value of α at which the shearing direction changes, γ_o is the plastic shear strain at the point α_o being defined, α_f is given by $\alpha_f = \tan\theta_{\alpha f}$ as shown in Fig.5 in which M_{fcomp} and M_{fext} are the effective stress rations at the failure state for compression and extension, respectively, α_m is the value of α at $\eta = M_m$, γ_m is the plastic shear strain at $\eta = M_m$, ξ_o and ξ^*_o are the parameters which define the magnitude of expansion and shrinkage of elastic regions. In the case of cyclic loading, the increase of α dependent on the plastic strain is calculated by folding the monotonic loading curve I-I as shown in Fig.4.

Fig.6 shows the experimental results obtained from the drained cyclic triaxial test of normally consolidated sand. The full lines show the most likely exponential curve fitted to the experimental results which are shown by symbols. The initial tangent of curve, that is ξ_o, becomes larger as the void ratio of sample becomes smaller. This

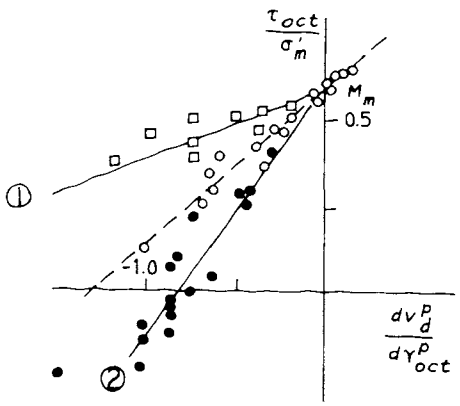

Fig.3 Stress-Dilatancy Relation

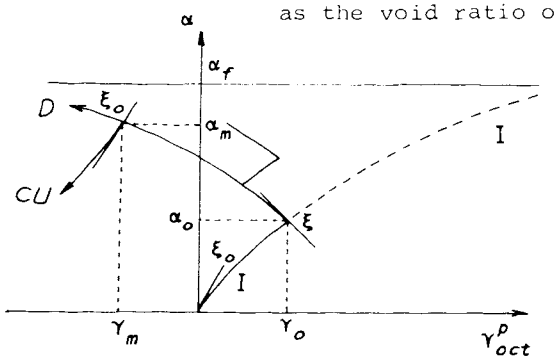

Fig.4 Isotropic Hardening Function

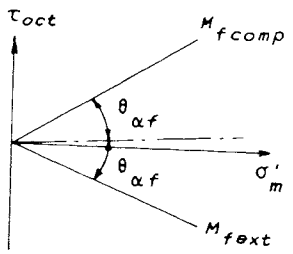

Fig.5 Definition of α_f

means that the rate of enlargement of the elastic region is larger in the case of denser sand and ξ_o is expressed as a function of density. At the beginning of shear deformation, α has a non-zero value. This suggests that the normally consolidated sand is not on the virgin consolidation line but it is on the over consolidated state.

(4) The Kinematic Hardening Rule

To define the measure of kinematic hardening, it is necessary to introduce another assumption of η-γ^p_{oct} relation which is expressed by a hyperbolic function as follows:

$$\eta-\eta_o=\frac{(AM_f-\eta_o)G'(\gamma^p_{oct}-\gamma_o)}{(AM_f-\eta_o)+G'(\gamma^p_{oct}-\gamma_o)} \qquad (13)$$

where $G'=(OCR)^{\frac{1}{2}}G_c$, G_c is the initial tangent modulus in η-γ^p_{oct} curve of a normally consolidated sand.

There are no firm experimental results for expressing the η-γ^p_{oct} curve by a hyperbolic function. However there is an advantage that the hardening function can be easily formulated in terms of two basic parameters of soil.

The restriction of continuing the plastic deformation is given by $df^*_s=0$. Substituting the relation $f^*_s=\eta-\eta^{\pm}_y$ in this equation, the following equation results

$$d\eta-\frac{\partial\eta^{\pm}_y}{\partial\alpha}d\alpha-\frac{\partial\eta^{\pm}_y}{\partial\beta}d\beta=0 \qquad (14)$$

Considering the relationship given by Eqs.(11), (12) and (13), we can get the differential equation for the kinematic hardening parameter β with respect to the plastic shear strain:

$$\frac{d\beta}{d\gamma^p_{oct}}=\left(\frac{d\eta}{d\gamma^p_{oct}}-\frac{\partial\eta^{\pm}_y}{\partial\alpha}\frac{d\alpha}{d\gamma^p_{oct}}\right)\Big/\left(\frac{\partial\eta^{\pm}_y}{\partial\beta}\right) \qquad (15)$$

(5) Hardening Functions

The hardening function h_c for consolidation is expressed by the assumption of isotropic hardening and non-recoverable volumetric strain component

$$h_c=\frac{\lambda-\kappa}{1+e}\frac{d\sigma'_m}{\sigma'_m} \qquad (16)$$

where λ and κ are the slope of the virgin compression line and of the swelling line in the e-$ln\sigma'_m$ plane and e is the void ratio.

The hardening function for shear deformation h_s is derived from Eqs. (1) and (14). Using Eqs.(1) and (8), we can get the following expression for plastic octahedral shearing strain increment

$$d\gamma^p_{oct}=\frac{2}{3}h_s\frac{\partial g_s}{\partial\tau_{oct}}df_s=\frac{2}{3}h_s d\eta \qquad (17)$$

Substituting Eqs.(14) and (15) into Eq.(17), the hardening function results as follows:

$$h_s=\frac{2}{3}\frac{1}{\left(\frac{\partial\eta^{\pm}_y}{\partial\alpha}\frac{d\alpha}{d\gamma^p_{oct}}+\frac{\partial\eta^{\pm}_y}{\partial\beta}\frac{d\beta}{d\gamma^p_{oct}}\right)} \qquad (18)$$

UNDRAINED CYCLIC TRIAXIAL STRESS PATH

For the undrained condition it is necessary to put a restriction for deformation so that the total incremental volumetric strain should be zero:

$$dv=dv^p_d+dv^p_c \qquad (19)$$

where dv^p_d and dv^p_c are calculated from Eqs.(1),(16) and (18) as follows:

$$dv^p_d=h_sB(AM_m-\eta)d\eta$$
$$dv^p_c=h_c d\sigma'_m \qquad (20)$$

Substituting Eq.(20) into Eq.(19), the effective stress increment $d\sigma'_m$ can be obtained

$$d\sigma'_m=\frac{h_s}{h_c}B(AM_m-\eta)d\eta \qquad (21)$$

Because Eq.(21) generally can not be integrated directly, a simple numerical procedure has been used in calculating the behaviour. Eq.(21) defines $d\sigma'_m/d\eta$ at the current value of η. The value of σ'_m at the adjacent point $\eta+d\eta$ is calculated as follows:

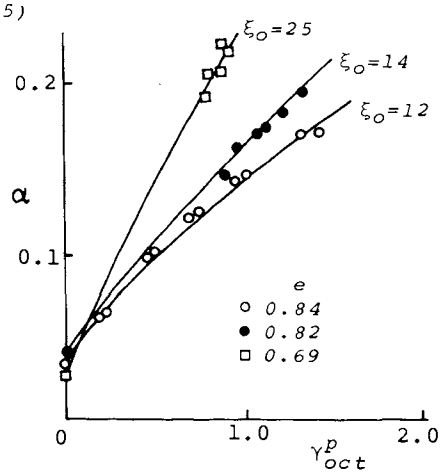

Fig.6 α-γ^p_{oct} Relationship

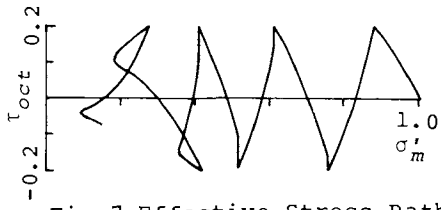

Fig.7 Effective Stress Path (ξ_o=10, unit:kg/cm^2)

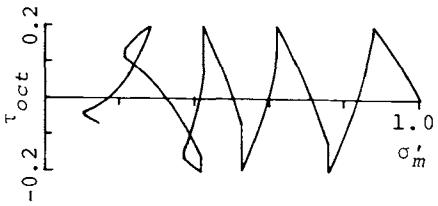

Fig.8 Effective Stress Path (ξ_o=20, unit:kg/cm^2)

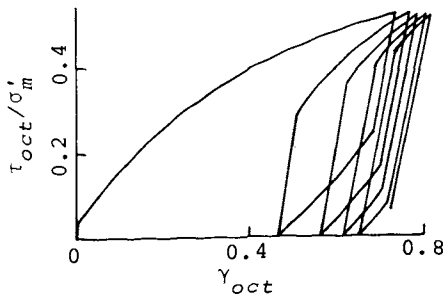

Fig.9 η-γ_{oct} Relationship (Simulation, ξ_o=14)

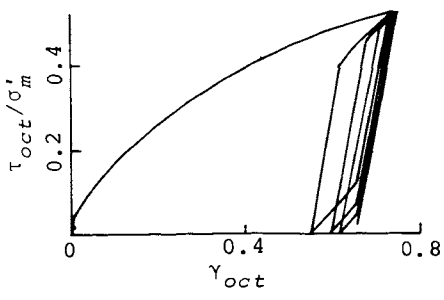

Fig.10 η-γ_{oct} Relationship (Simulation, ξ_o=25)

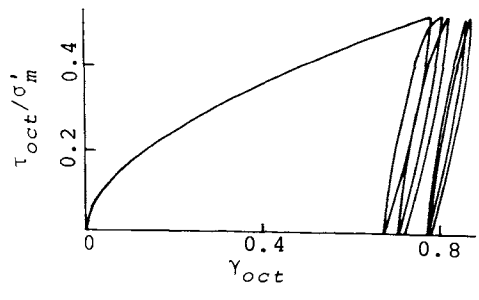

Fig.11 η-γ_{oct} Relationship (Experimental result)

$$(\sigma'_m)_{i+1} = (\sigma'_m)_i + \left(\frac{d\sigma'_m}{d\eta}\right)_i d\eta$$

The undrained cyclic triaxial stress paths under the condition of constant τ_{oct} amplitude are shown in Figs.7 and 8. The dynamic properties used for the calculation are listed in Table 1. From these figures it is clear that the proposed model can express the generally recognized experimental phenomenon that the excess pore pressure accumulates as the cyclic process proceeds. Moreover, if the effective stress ratio exceeds the phase transformation line (M_m-line), which is obtained from the angle of phase transformation ϕ_m, the accumulation pattern of excess pore pressure changes drastically (called as the initial liquefaction). After this phenomenon appears, the large excess pore pressure is developed. The straight line parts of stress path parallel to the vertical axis are the elastic regions which expand as the number of repetitions increases and shrink after the occurence of the initial liquefaction. The accumulation of pore pressure in each cycle decreases as the value of ξ_o increases.

DRAINED CYCLIC TRIAXIAL TEST

In the case of monotonic loading, it might be possible to assume that the strain developed by the increment of stress is mainly from the plastic deformation. However, in the case of cyclic loading, we have to evaluate correctly the magnitude of recovering strain on the unloading process and of residual strain at the end of the unloading process.

Figs.9 and 10 show the simulated stress-strain relationship of the drained triaxial cyclic loading test for ξ_o as 14.0 and 25.0, respectively. The material properties used for calculation are the same given in Table 1. The results bear an encouraging similarity to the experimental results shown in Fig.11. The numerical results overestimate the recovering shear strain, however, the expanding process of elastic region with the increase of the repetition are expressed precisely.

THE STRESS-DILATANCY RELATIONSHIP UNDER CYCLIC LOADING

In this analysis, the effective stress ratio M_m is assumed as a unique property of sand unaffected by stress history. This is admissible for the case of monotonic loading. We check here the validity of this assumption by using cyclic loading test results. Fig.12 shows a typical experimental results in which the amplitude of octahedral shear stress was changed five times. On each stress level five cycles of repetition were applied to the specimen. This figure shows the volume change-τ_{oct} relation. The stress ratio applied to the specimen exceeds M_m around point *4*, so the characteristic of volume change turns from shrinkage to expansion. This phenomenon becomes more predominant in the first loading cycle of the next stress level (*5-6-7*). However, the volume change at the end of the fifth repetition becomes very small because the elastic region expands to the stress level of point *8*. This means that the value of M_m is pushed up by the cyclic stress history exceeding the initial M_m-line.

To make clear this argument, the stress-dilatancy relationship is shown in Fig.13. The intersection with the vertical axis, which defines the value of M_m, becomes large as the stress level of cyclic loading increases. In this figure we can also see the effect of anisotropic consolidation on the stress-dilatancy relationship, that is, the slope of the relationship becomes gentle as the stress ratio η becomes large.

Table 1. Material Properties

G_o=600, G_e=800, λ=0.0015, κ=0.005					
M_f	comp.	0.837	M_m	comp.	0.576
	ext.	0.538		ext.	0.409

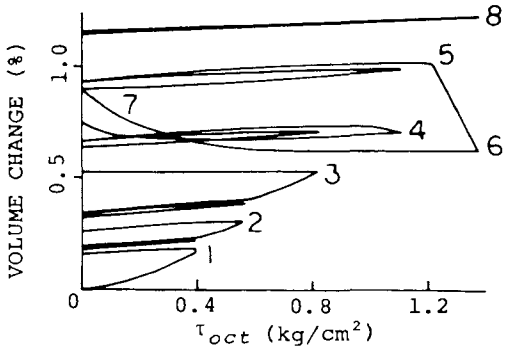

Fig.12 Volume Change-τ_{oct} Relationship

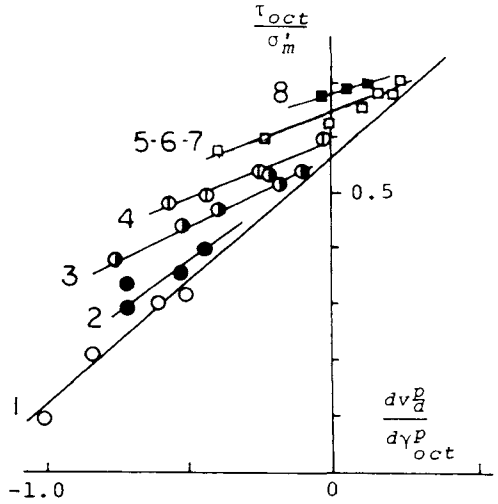

Fig.13 Stress-Dilatancy Relationship

CONCLUSION

A new mathematical model has been proposed to present the stress-strain behaviour of sandy soil under cyclic loading conditions. The theory was based on a non-associated flow rule. The kinematic and isotropic hardening rules were fundamental concepts to formulate the yield and hardening function. The plastic potential was derived from the stress-dilatancy relationship including the effect of anisotropic consolidation. The results of numerical calculations showed the advantage of providing a highly unified treatment of stress-strain behaviour of saturated sand.

REFERENCES

1) Roscoe,K.H. and Burland,J.B.; Engineering Elasticity, Cambridge Univ. Press, 1968.
2) Morz,Z.,Norris,V.A. and Zienkiwicz,O.C.; Geotechnique,Vol.24,pp.1-34,1979.
3) Hill,R.; The Mathematical Theory of Plasticity, Oxford Univ. Press, 1950.
4) Sato,T.,Shibata,T. and Kosaka,M.; Inter.Symp. Soil under Cyclic and Transient Loading, pp. 523-532, 1980.